Study on $\eta_{c2}(\eta_{b2})$ electromagnetic decay into double photons

Li Yang,[1] Wen-Long Sang,[1,*] Hong-Fei Zhang,[2,†] Yu-Dong Zhang,[1] and Ming-Zhen Zhou[1,‡]

[1]*School of Physical Science and Technology, Southwest University, Chongqing 400700, China*
[2]*College of Big Data Statistics, Guizhou University of Finance and Economics, Guiyang 550025, China*

(Received 29 October 2020; accepted 2 February 2021; published 24 February 2021)

Within the framework of nonrelativistic QCD factorization formalism, we compute the helicity amplitude as well as the decay width of η_{Q2} ($Q = c$, b) electromagnetic decay into two photons up to next-to-next-to-leading order in α_s expansion. For the first time, we verify the validity of nonrelativistic QCD factorization for the D-wave quarkonium decay at next-to-next-to-leading order. We find that the $\mathcal{O}(\alpha_s)$ and $\mathcal{O}(\alpha_s^2)$ corrections to the helicity amplitude are negative and moderate, nevertheless both corrections combine to suppress the leading-order prediction for the decay width significantly. By approximating the total decay width of η_{Q2} as the sum of those for the hadronic decay and the electric $E1$ transition, we obtain the branching ratios $\mathrm{Br}(\eta_{c2} \to 2\gamma) \approx 5 \times 10^{-6}$ and $\mathrm{Br}(\eta_{b2} \to 2\gamma) \approx 4 \times 10^{-7}$. To explore the potential measurement on η_{Q2}, we further evaluate the production cross section of η_{Q2} at LHCb at the lowest order in α_s expansion. With the kinematic constraint on the longitudinal rapidity $4.5 > y > 2$ and transverse momentum $P_T > (2\text{–}4)m_Q$ for η_{Q2}, we find the cross section can reach 2–50 nb for η_{c2}, and 1–22 pb for η_{b2}. Considering the integrated luminosity $\mathcal{L} = 10\ \mathrm{fb}^{-1}$ at $\sqrt{s} = 7$, 13 TeV, we estimate that there are several hundreds events of $pp \to \eta_{c2} \to 2\gamma$. Since the background is relatively clean, it is promising to reconstruct η_{c2} through its electromagnetic decay. On the other hand, due to the small branching ratio and production cross section, it is quite challenging to detect $\eta_{b2} \to 2\gamma$ at LHCb.

DOI: 10.1103/PhysRevD.103.034018

I. INTRODUCTION

Heavy quarkonium, as a multiscale system, is an ideal laboratory for testing the interplay between perturbative and nonperturbative QCD. Its mass spectrum has been predicted by various potential models, and most of the low-lying quarkonium states have been probed by the experiment. However there still exist some undiscovered states. Among the missing states in charmonium family, $\eta_{c2}(^1D_2)$ is the only spin-singlet low-lying D-wave state. A full understanding on η_{c2} in both theory and experiment can help to illuminate the interquark force and reveal the nature of the strong interaction.

The mass of η_{c2} is predicted to range from 3.80 to 3.88 GeV [1–7], which lies between the $D\bar{D}$ and the $D^*\bar{D}$ thresholds. Quite different from ψ'', the decay of η_{c2} into $D\bar{D}$ is forbidden, which is accounted for by the parity conservation. Thus η_{c2} is a narrow resonance, and its main decay modes are considered to be hadronic decay and electric $E1$ transition, which have been well investigated in the references.

The electric $E1$ transition has been known for a long time [2,7,8] (see also the review in [9]). The hadronic transition $\eta_{c2} \to \pi\pi\eta_c$ was evaluated in Ref. [8]. The η_{c2} hadronic decay was studied in Refs. [10,11]. Production through B meson decay is an important channel to search for charmonia [12–17]. Based on the nonrelativisitc QCD (NRQCD) factorization formalism [18], the inclusive η_{c2} production in B decay was evaluated and proposed to probe η_{c2} through this channel [19,20]. The decay $B^- \to \eta_{c2}K^-$ has been explored by using the rescattering mechanism in Ref. [21]. In addition, the η_{Q2} electromagnetic decay into double photons was evaluated by using the instantaneous Bethe-Salpeter method in Ref. [22]. Unfortunately, no significant signal has been found till today [23].

The $C = +1$ charmonia bear a considerable branching ratio of electromagnetic decay into double photons, e.g., $\mathrm{Br}(\eta_c \to 2\gamma) \approx 1.57 \times 10^{-4}$, $\mathrm{Br}(\chi_{c0} \to 2\gamma) \approx 2.04 \times 10^{-4}$, and $\mathrm{Br}(\chi_{c2} \to 2\gamma) \approx 2.85 \times 10^{-4}$ [24], which have been well measured by the experiment. Although the electric $E1$ transition $\eta_{c2} \to h_c\gamma$ comprises one of the main decay channel, it is anticipated that the branching ratio for η_{c2} electromagnetic decay is of the same magnitude as those in

*Corresponding author.
wlsang@swu.edu.cn
†shckm2686@163.com
‡zhoumz@swu.edu.cn

η_c and χ_c. Compared with the hadronic decay, the electromagnetic decay has the advantage of bearing a clean background. Thus we propose to detect η_{c2} through $\eta_{c2} \to 2\gamma$. In this work, we will evaluate the partial width of $\eta_{Q2} \to 2\gamma$ (the heavy quark flavor $Q = c, b$) within the framework of the well-established NRQCD factorization formalism.

NRQCD factorization formalism is widely employed to tackle heavy quarkonium decay and production. Within this framework, the production cross section or decay width can be systematically disentangled the short-distance and long-distance effects, formalized by a double expansion in powers of heavy quark velocity v_Q and strong coupling constant α_s. The perturbative contributions with the scale larger than the heavy quark m_Q is encoded into the short-distance coefficients (SDCs), while the nonperturbative effects are contained in the NRQCD long-distance matrix elements (LDMEs).

Recently, there is a remarkable progress in deducing the higher-order perturbative corrections for various quarkonium decay and production processes [25–41]. It has been found even though the $\mathcal{O}(\alpha_s)$ corrections to the charmonium electromagnetic decay are moderate, the $\mathcal{O}(\alpha_s^2)$ corrections can be considerable. Therefore it is mandatory to include the $\mathcal{O}(\alpha_s^2)$ contributions in our evaluation. Concretely speaking, we will evaluate the decay width of $\eta_{Q2} \to 2\gamma$ up to next-to-next-to-leading order (NNLO) in perturbative α_s expansion.

In addition, to provide aid for experimental search for η_{Q2} through $\eta_{Q2} \to 2\gamma$, we will explore the η_{Q2} production at colliders, and estimate the corresponding number of events. The η_{c2} associated production with a photon at B factory has been obtained in Ref. [42]. The $\eta_{c2} + J/\psi$ production at B factory can be found in Ref. [43]. Unfortunately, the cross sections of both channels are too small to probe $\eta_{c2} \to 2\gamma$. Considering the significant luminosity as well as the sizeable cross sections for quarkonia production at LHC, exemplified by $\sigma(pp \to \eta_c + X) \sim 0.5\ \mu\text{b}$ with the transverse momentum cut $p_T > 4m_c$ [44], we anticipate the cross section for η_{c2} production is also considerable. Actually, the cross section of η_{c2} at LHC can be simply estimated by $\sigma(\eta_{c2}) \sim \frac{|\mathcal{R}_D''(0)|^2}{m_c^4 |\mathcal{R}_S(0)|^2} \times \sigma(\eta_c) \sim v_c^4 \times 0.5\text{–}5\,\text{nb}$. Thus, we expect that there are a number of events for $pp \to \eta_{c2} \to 2\gamma$, which renders $\eta_{c2} \to 2\gamma$ a promising channel to probe η_{c2}.

The remainder of this paper is organized as follows. In Sec. II, we make a Lorentz decomposition for the amplitude of $\eta_{Q2} \to 2\gamma$, and present the decay width in term of the helicity amplitudes. In Sec. III, we outline the NRQCD factorization formalism for the helicity amplitude, and briefly describe the theoretical framework to deduce the NRQCD SDC. In Sec. IV, we first introduce the technicalities encountered in performing loop calculation, and then present our final results for the SDC. Section V is devoted to the phenomenological analysis and discussion. A theoretical prediction on the production cross section of η_{Q2} at LHCb is also contained in this section. We present our summary in Sec. VI.

II. THEORETICAL FORMULA FOR THE DECAY WIDTH

The partial width of $\eta_{Q2} \to 2\gamma$ can be expressed in term of helicity amplitude

$$\Gamma_{\gamma\gamma}(\eta_{Q2}) = \frac{1}{2J+1} \frac{1}{2!} \frac{1}{8\pi} [2|\mathcal{A}_{1,1}|^2 + 2|\mathcal{A}_{1,-1}|^2], \quad (1)$$

where $J = 2$ denotes the spin of η_{Q2}, $\frac{1}{2!}$ accounts for the indistinguishability of the two identical photons, $\frac{1}{8\pi}$ corresponds to the phase space factor, and $\mathcal{A}_{\lambda_1,\lambda_2}$ signifies the helicity amplitudes of $\eta_{Q2} \to \gamma(\lambda_1)\gamma(\lambda_2)$ with $\lambda_{1,2} = \pm 1$ being the helicity of the photons. By invoking the parity invariance, we only enumerate the independent helicity amplitudes.[1]

To extract the helicity amplitudes, we first decompose the amplitude $\mathcal{A}$ of $\eta_{Q2} \to 2\gamma$ by Lorentz invariance. By Bose symmetry, the transversality for the polarization of photons, together with the parity conservation, the amplitude can be generically expressed as

$$\begin{aligned}
\mathcal{A} = {} & \frac{c_1}{m_Q^4} \epsilon^{\alpha\beta\rho\sigma} \epsilon_{1\alpha}^* \epsilon_{2\beta}^* k_{1\rho} p_\sigma k_{1\mu} k_{1\nu} \epsilon_H^{\mu\nu} \\
& + \frac{c_2}{m_Q^2} \epsilon^{\alpha\beta\mu\rho} \epsilon_{1\alpha}^* \epsilon_{2\beta}^* p_\rho \epsilon_{H\mu\nu} k_1^\nu \\
& + \frac{c_3}{m_Q^2} (\epsilon^{\alpha\mu\rho\sigma} \epsilon_{1\alpha}^* k_{1\rho} p_\sigma \epsilon_{H\mu\nu} \epsilon_2^{*\nu} \\
& - \epsilon^{\alpha\mu\rho\sigma} \epsilon_{2\alpha}^* k_{1\rho} p_\sigma \epsilon_{H\mu\nu} \epsilon_1^{*\nu}),
\end{aligned} \quad (2)$$

where p denotes half of the momentum of η_{Q2}, k_1 and k_2 signify the momenta of the two outgoing photons, c_i ($i = 1, 2, 3$) are Lorentz invariants and refer to form factors of the corresponding Lorentz structure, ϵ_1 and ϵ_2 represent the polarization vectors of the photons, and ϵ_H denotes the polarization tensor of η_{Q2}.

It is straightforward to deduce the helicity amplitudes $\mathcal{A}_{\lambda_1,\lambda_2}$ from Eq. (2). To carry out the calculation, it is convenient to construct the explicit expressions of the polarization tensor ϵ_H and polarization vectors ϵ_1 and ϵ_2 [46]. We define the polarization vectors

[1]Note that the relation $\mathcal{A}_{\lambda_1,\lambda_2} = (-1)^J \mathcal{A}_{\lambda_2,\lambda_1}$, which is constrained by the exchange symmetry for the two identical photons, and the P parity further enforces the restriction $\mathcal{A}_{\lambda_1,\lambda_2} = -\mathcal{A}_{-\lambda_1,-\lambda_2}$ for η_{Q2} [45], therefore we have $\mathcal{A}_{1,-1} = -\mathcal{A}_{1,-1} = 0$. We will demonstrate the vanishment of $\mathcal{A}_{1,-1}$ through an explicit evaluation in the following.

$$\epsilon_+^\mu = \frac{1}{\sqrt{2}}(0,-1,-i,0), \qquad \epsilon_-^\mu = \frac{1}{\sqrt{2}}(0,+1,-i,0),$$
$$\epsilon_0^\mu = (0,0,0,1). \tag{3}$$

The five polarization tensors of η_{Q2} are readily expressed as

$$\epsilon_{H\pm2}^{\mu\nu} = \epsilon_\pm^\mu \epsilon_\pm^\nu, \tag{4a}$$

$$\epsilon_{H\pm1}^{\mu\nu} = \frac{1}{\sqrt{2}}(\epsilon_\pm^\mu \epsilon_0^\nu + \epsilon_0^\mu \epsilon_\pm^\nu), \tag{4b}$$

$$\epsilon_{H\pm0}^{\mu\nu} = \frac{1}{\sqrt{6}}(\epsilon_+^\mu \epsilon_-^\nu + 2\epsilon_0^\mu \epsilon_0^\nu + \epsilon_-^\mu \epsilon_+^\nu). \tag{4c}$$

If assuming the photon with momentum k_1 is outgoing in the positive z direction, its polarization vector ϵ_1 equals to ϵ_+ for helicity $+1$, and ϵ_- for helicity -1, while the helicity polarization vector of the backward photon is just reversed.

Substituting the explicit expressions Eqs. (3) and (4) into Eq. (2), we obtain the helicity amplitudes in term of the three form factors

$$\mathcal{A}_{1,1} = -\frac{2i}{\sqrt{6}}(c_1 - c_2 + c_3), \tag{5a}$$

$$\mathcal{A}_{1,-1} = 0, \tag{5b}$$

where $\mathcal{A}_{1,-1}$ explicitly vanishes.

III. NRQCD FACTORIZATION FORMALISM FOR THE HELICITY AMPLITUDE

Owing to the strong interaction inner the hadron η_{Q2}, the helicity amplitude $\mathcal{A}_{1,1}$ is nonperturbative. Fortunately, we can employ the NRQCD factorization formalism to factorize the helicity amplitude into [18]

$$\mathcal{A}_{1,1} = \mathcal{C}_{1,1}(\mu_F)\frac{\langle 0|\chi^\dagger \mathcal{K}_{^1D_2}\psi(\mu_F)|\eta_{Q2}\rangle}{m_Q^{5/2}}(1+\mathcal{O}(v^2)), \tag{6}$$

where $\mathcal{C}_{1,1}$ represents the perturbative SDC, which depicts a heavy quark pair annihilation into double photons, μ_F signifies the factorization scale, and

$$\mathcal{K}_{^1D_2} = \left(-\frac{i}{2}\right)^2 \left(\overleftrightarrow{D}^i \overleftrightarrow{D}^j - \frac{1}{3}\overleftrightarrow{\boldsymbol{D}}^2 \delta^{ij}\right)\epsilon_H^{ij}, \tag{7}$$

with ϵ_H being the polarization tensor of η_{Q2}. LDME $\langle 0|\chi^\dagger \mathcal{K}_{^1D_2}\psi(\mu_F)|\eta_{c2}\rangle$ deciphering the nonperturbative effect in the hadron is process independent, and can be related to the second derivative of the radial wave function at the origin through

$$\langle 0|\chi^\dagger \mathcal{K}_{^1D_2}\psi(\mu_F)|\eta_{Q2}\rangle = \sqrt{\frac{5N_c}{8\pi}}\overline{\mathcal{R}''_D}(\mu_F), \tag{8}$$

where the wave functions at the origin should be promoted as a scale-dependent quantity in the field theoretical context. For simplicity, we will suppress the μ_F dependence in SDC and LDME when it will not bring confusion.

To get the helicity amplitude, we must determine the SDC. Since the SDC is irrelevant to the nonperturbative hadronization effect, it can be computed through the standard matching technique. Concretely, we can replace the physical meson η_{Q2} with a heavy quark pair $Q\bar{Q}$, carrying the same quantum number as $^1D_2$. The factorization formalism is also valid to the free quark state $Q\bar{Q}(^1D_2)$, therefore after the replacement, Eq. (6) becomes

$$\mathcal{A}_{1,1}(^1D_2) = \mathcal{C}_{1,1}\frac{\langle 0|\chi^\dagger \mathcal{K}_{^1D_2}\psi|Q\bar{Q}(^1D_2)\rangle}{m_Q^{5/2}}, \tag{9}$$

where we have suppressed the factorization scale and the high-order relativistic corrections. The SDC in Eq. (9) is exactly the same as in Eq. (6). Since the amplitude $\mathcal{A}_{1,1}$ and matrix element are now perturbative, both sides of Eq. (9) are calculable. In principle, one can solve the SDC $\mathcal{C}_{1,1}$ in any prescribed α_s order.

In the following, we briefly describe the procedure to evaluate the perturbative helicity amplitude $\mathcal{A}_{1,1}(^1D_2)$. We assign the momenta of the Q and $\bar{Q}$ quarks to be

$$p_1 = p + q,$$
$$p_2 = p - q, \tag{10}$$

where p and q represent half of the total momentum and the relative momentum of the $Q\bar{Q}$ pair, respectively. The on shell condition enforces that

$$p^2 = p_1^2 = p_2^2 = m_Q^2,$$
$$p\cdot q = 0. \tag{11}$$

In our calculation, we first evaluate the amplitude $\mathcal{A}$ of $Q\bar{Q}\to 2\gamma$, then employ the covariant spin projector to extract the spin-singlet component of the $Q\bar{Q}$. To be consistent with the decay width formula (1), we utilize the nonrelativistically normalized spin-singlet/color-singlet projector [47], which reads

$$\Pi_0 = \frac{(\not{p}+\not{q}+m_Q)(\not{p}+m_Q)\gamma_5(\not{p}-\not{q}-m_Q)}{8\sqrt{2}m_Q^3}\otimes\frac{\mathbf{1}_c}{\sqrt{N_c}}. \tag{12}$$

The $L=2$ orbital partial wave can be projected out by differentiating the color-singlet/spin-singlet quark amplitude with respect to the relative momentum q, followed by setting q to zero

$$\mathcal{A}(^1D_2) = \epsilon_{H\mu\nu} \frac{|\mathbf{q}|^2}{2!} \frac{\partial^2}{\partial q_\mu \partial q_\nu} \mathrm{Tr}[\Pi^0 \mathcal{A}]|_{q=0}. \tag{13}$$

Now, we have collected all the necessary ingredients to calculate the amplitude of $Q\bar{Q}(^1D_2) \to 2\gamma$. Subsequently, we can pick up the Lorentz invariant form factor c_i through Eq. (2), and obtain the perturbative helicity amplitude with the aid of Eq. (5). Meanwhile, the perturbative NRQCD matrix element $\langle 0|\chi^\dagger \mathcal{K}_{^1D_2}\psi|Q\bar{Q}(^1D_2)\rangle$ can also be carried out at a desired α_s order. At lowest order in α_s, we have

$$\langle 0|\chi^\dagger \mathcal{K}_{^1D_2}\psi|Q\bar{Q}(^1D_2)\rangle = \sqrt{2N_c}|\mathbf{q}|^2. \tag{14}$$

Finally, it is straightforward to determine the SDC $\mathcal{C}_{1,1}$ at a prescribed α_s order through Eq. (9).

For the future convenience, we reexpress the partial width of $\eta_{Q2} \to 2\gamma$ in terms of the SDC

$$\Gamma_{\gamma\gamma}(\eta_{Q2}) = \frac{1}{5}\frac{1}{8\pi}|\mathcal{C}_{1,1}|^2 \frac{|\langle 0|\chi^\dagger \mathcal{K}_{^1D_2}\psi|\eta_{c2}\rangle|^2}{m_Q^5}. \tag{15}$$

IV. SDC UP TO NNLO

In this section, we first describe the computational technicalities utilized to evaluate the perturbative amplitude in detail, then present our main results for the SDC $\mathcal{C}_{1,1}$.

We employ FeynArts [48] to generate the Feynman diagrams and the corresponding amplitude for $Q\bar{Q} \to 2\gamma$. The representative Feynman diagrams are illustrated in Fig. 1. We employ the spin-singlet/color-singlet projector (12) and apply the recipe as specified in (13) to project out the intended amplitude for $Q\bar{Q}(^1D_2) \to 2\gamma$ up to two-loop level. Subsequently, the packages FeynCalc [49,50] and FormLink [51,52] are employed to perform the Dirac trace and Lorentz contraction.

For the NLO and NNLO corrections, we carry out the derivative of the amplitude with regard to the relative momentum q prior to perform loop integration, which amounts to directly extract the contribution from the hard region. We employ the package APART [53] and FIRE [54] to conduct partial fraction and the corresponding integration-by-part reduction. Finally, we have 3 one-loop master integrals (MIs) and 80 two-loop MIs. There exist some complex-valued two-loop integrals originating from the $gg \to \gamma\gamma$ subprocess (since their Feynman diagrams are of the same topological structure as the well-known light-by-light scattering for two photons, in this work, we will call this class of diagrams light-by-light (lbl), as illustrated in Fig. 1, which are relatively hard to carry out numerically. It deserves mentioning that although the MIs encountered here are almost the same sets as in the processes $\eta_c \to 2\gamma$ and $\chi_c \to 2\gamma$, the computation complexity is much more involved. Since we have taken the second derivative of the amplitude with respect to the relative momentum q, some coefficients of the MIs are relatively larger as well as more divergent in $1/\epsilon$ expansion compared with those in η_c and χ_c decay. Thus, to reach the desired precision, we must perform numerical integration over the MIs to higher accuracy.

For the real-valued MIs, we directly use CUBPACK/HCUBATURE [55,56] to carry out the integration. In contrast to the application of sector decomposition to the Euclidean region, the singularities encountered in the physical region lie inside, rather than sit on, the integration boundary, which renders the integration hard to be numerically evaluated. To overcome this difficulty, we conduct integration contour deformation via the variable transformation prior to decomposing the sectors [57], and determine the integration contour through optimizing a set of contour parameters [38]. For more technical details, we refer the readers to Refs. [38,41].

The lbl Feynman diagrams are both gauge invariant and free of any UV and IR divergences in sum. In contrast, for the non-lbl diagrams, there exist UV divergence at one loop, and both UV and IR divergences at two loop. The UV divergence originates from the integration over the loop

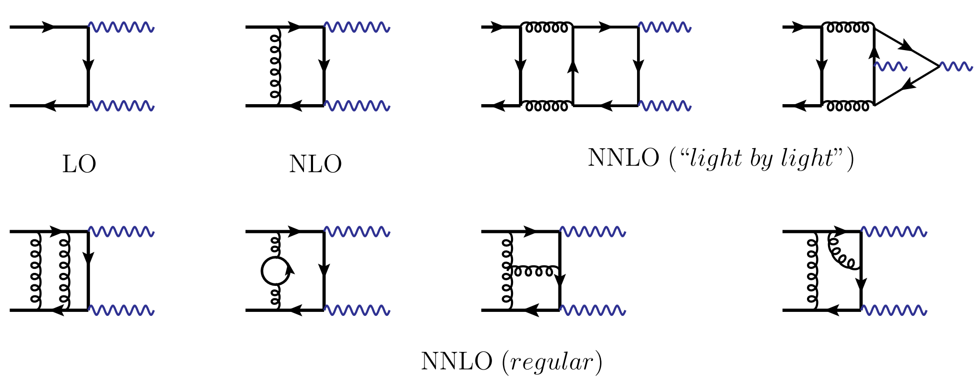

FIG. 1. The representative Feynman diagrams for $Q\bar{Q}(^1D_2) \to 2\gamma$ through order α_s^2.

momentum, which can be eliminated through the standard renormalization procedure. We implement the on shell renormalization for the heavy quark wave function and mass up to $\mathcal{O}(\alpha_s^2)$ [58–60], and $\overline{\mathrm{MS}}$ renormalization for the strong coupling constant. Thus, the ultimate amplitude is completely UV finite. There remains a piece of unremoved IR divergence, nevertheless this IR pole can be factored into the NRQCD LDME, so that the NRQCD SDC becomes IR finite. As a consequence, both of the LDME and the corresponding two-loop SDC $\mathcal{C}_{1,1}$ bear $\ln\mu_F$ dependence, nevertheless their product must be independent of factorization scale through $\mathcal{O}(\alpha_s^2)$.

After some hard work, we finally obtain the SDC $\mathcal{C}_{1,1}$ expanded in power of the strong coupling constant α_s

$$\mathcal{C}_{1,1} = \frac{4\sqrt{6}\pi}{3\sqrt{m_Q}}\alpha e_Q^2\left\{1 + C_F\frac{\alpha_s}{\pi}\Delta^{(1)} + \frac{\alpha_s^2}{\pi^2}\left[C_F\frac{\beta_0}{4}\Delta^{(1)}\ln\frac{\mu_R^2}{m_Q^2} + \Delta^{(2)}\right]\right\}, \quad (16)$$

where α denotes the electromagnetic coupling constant, e_Q signifies the electric charge of the heavy quark, $\beta_0 = \frac{11}{3}C_A - \frac{2}{3}(n_L + n_H)$ corresponds to the one loop coefficient of the QCD β function, where $n_H = 1$, and n_L signifies the number of the active quark flavor ($n_L = 3$ for η_{c2}, and $n_L = 4$ for η_{b2}), and $C_F = \frac{4}{3}$, $C_A = 3$ are $SU(3)$ color factors. The exact occurrence of the $\ln\mu_R^2$ is demanded by the renormalization group invariance.

$\Delta^{(1)}$ and $\Delta^{(2)}$ correspond to the $\mathcal{O}(\alpha_s)$ and $\mathcal{O}(\alpha_s^2)$ corrections to the SDC. The expression of $\Delta^{(1)}$ is analytically obtained

$$\Delta^{(1)} = \frac{3}{8}\pi^2 - 6\ln 2 - 1. \quad (17)$$

$\Delta^{(2)}$ can be expressed as

$$\Delta^{(2)} = -\frac{\pi^2}{10}C_F(C_A + 2C_F)\ln\frac{\mu_F}{m_Q} + \Delta^{(2)}_{\mathrm{reg}} + \Delta^{(2)}_{\mathrm{lbl}}. \quad (18)$$

The coefficient of the factorization scale dependence $\ln\mu_F$ term corresponds to the anomalous dimension of the NRQCD operator in Eq. (6), which is consistent with the result in Ref. [61],[2] and thereby the NRQCD factorization is verified in η_{Q2} electromagnetic decay. The terms of $\Delta^{(2)}_{\mathrm{reg}}$ and $\Delta^{(2)}_{\mathrm{lbl}}$ in (18) represent the contributions from the regular and "light-by-light" Feynman diagrams, which are illustrated in Fig. 1.

[2] In Ref. [61], the authors computed the anomalous dimensions of spin-single and spin-triplet currents for heavy quark pair with arbitrary orbital angular momentum. The anomalous dimension of ${}^1D_2$ can be obtained by utilizing Eq. (40) in Ref. [61] with color-singlet Wilson coefficients of the potentials given in Refs. [62–65].

Furthermore, we can organize the $\Delta^{(2)}_{\mathrm{reg}}$ and $\Delta^{(2)}_{\mathrm{lbl}}$ according to the color structure,

$$\Delta^{(2)}_{\mathrm{reg}} = C_F^2 s_A + C_F C_A s_{NA} + n_L C_F T_F s_L + n_H C_F T_F s_H, \quad (19)$$

where the color factor $T_F = \frac{1}{2}$,

$$s_A = -5.8455, \qquad s_{NA} = -4.3701,$$
$$s_L = 1.4464, \qquad s_H = 0.0161, \quad (20)$$

and

$$\Delta^{(2)}_{\mathrm{lbl}} = (0.0002 + 0.0056i)n_H C_F T_F + (0.2136 - 0.0082i)C_F T_F\sum_i^{n_L}\frac{e_i^2}{e_Q^2}, \quad (21)$$

where e_i represents the electric charge of the ith light flavor.

By setting the renormalization scale $\mu_R = m_Q$ and factorization scale $\mu_F = 1$ GeV, we get the radiative corrections to $\mathcal{C}_{1,1}$ at various perturbative orders,

$$\mathcal{C}_{1,1} = \frac{4\sqrt{6}\pi}{3\sqrt{m_Q}}\alpha e_Q^2(1 - 0.62\alpha_s - r\alpha_s^2), \quad (22)$$

where $r = 2.12 + 0.0005i$ for η_{c2} and $r = 1.11 + 0.005i$ for η_{b2}. We find that both the $\mathcal{O}(\alpha_s)$ and $\mathcal{O}(\alpha_s^2)$ corrections to the helicity amplitude are negative as well as moderate. It seems that the perturbative expansion for $\eta_{Q2} \to 2\gamma$ exhibits a decent convergence, however as will be found, the radiative corrections accurate up to $\mathcal{O}(\alpha_s^2)$ change the LO decay width considerably.

For completeness, it is necessary to deduce the explicit expression of decay width. Applying the formula Eq. (15) and the expression of helicity amplitude in Eq. (16), we readily obtain the decay width of $\eta_{Q2} \to 2\gamma$ through $\mathcal{O}(\alpha_s^2)$

$$\Gamma_{\gamma\gamma}(\eta_{Q2}) = \frac{4\pi\alpha^2 e_Q^4}{15}\frac{|\langle 0|\chi^\dagger\mathcal{K}_{{}^1D_2}\psi(\mu_F)|\eta_{c2}\rangle|^2}{m_Q^6} \times\left[1 + \frac{\alpha_s}{\pi}2C_F\Delta^{(1)} + \frac{\alpha_s^2}{\pi^2}\left(C_F^2\Delta^{(1)2} + C_F\frac{\beta_0}{2}\Delta^{(1)}\ln\frac{\mu_R^2}{m_Q^2} + 2\mathrm{Re}\Delta^{(2)}\right)\right], \quad (23)$$

where the symbol Re signifies the real part of the argument.

V. PHENOMENOLOGY

A. Predictions for the decay width

To make concrete prediction, we first choose the input parameters. We take the heavy quark mass to be

TABLE I. NRQCD predictions for the decay width of $\eta_{Q2}\to 2\gamma$ at various levels of accuracy in α_s. We take the two-loop quark pole masses $m_c = 1.68$ GeV and $m_b = 4.78$ GeV. The NRQCD LDMEs are evaluated by the Cornell potential model. The errors are estimated by sliding the renormalization scale μ_R from m_Q to $2m_Q$ with center value $\mu_R=\sqrt{2}m_Q$. By taking the total decay width as $\Gamma_{\text{total}}(\eta_c)\approx 445.1$ keV and $\Gamma_{\text{total}}(\eta_b)\approx 29.1$ keV, we also present the branching ratio $\text{Br}(\eta_{Q2}\to 2\gamma)$.

			$\mu_F = 1$ GeV		$\mu_F = m_Q$	
$\Gamma_{\gamma\gamma}$ in unit of eV	LO	NLO	NNLO	$\text{Br}(\eta_{Q2}\to 2\gamma)$	NNLO	$\text{Br}(\eta_{Q2}\to 2\gamma)$
$\eta_{c2}\to 2\gamma$	8.28	$5.68^{+0.25}_{-0.34}$	$2.61^{+0.70}_{-1.04}$	$5.9^{-2.3}_{+1.6}\times 10^{-6}$	$2.11^{+0.81}_{-1.23}$	$4.7^{-2.7}_{+1.8}\times 10^{-6}$
$\eta_{b2}\to 2\gamma$	0.025	$0.019^{+0.001}_{-0.001}$	$0.014^{+0.001}_{-0.001}$	$4.7^{-0.4}_{+0.3}\times 10^{-7}$	$0.011^{+0.001}_{-0.002}$	$3.9^{-0.5}_{+0.4}\times 10^{-7}$

$m_c = 1.68$ GeV and $m_b = 4.78$ GeV, which correspond to the two-loop charm quark and bottom quark pole masses converted from the corresponding $\overline{\text{MS}}$ masses [66]. We evaluate the electromagnetic coupling constant as $\alpha(2m_c)\approx\frac{1}{132}$ and $\alpha(2m_b)\approx\frac{1}{131}$ by the formulas in Ref. [67], and evaluate α_s at each energy scale by RunDec [66].

The NRQCD LDME is related to the second derivative of the 1D radial wave function at the origin in Eq. (8), which is well determined by the nonrelativistic potential model. From Eq. (8), we get

$$\begin{aligned}|\langle 0|\chi^\dagger\mathcal{K}_{^1D_2}\psi|\eta_{c2}\rangle|^2 &= \frac{5N_c}{8\pi}\overline{\mathcal{R}''_D}(\mu_F)^2\approx\frac{5N_c}{8\pi}\times 0.0329\\ &= 0.0196\ \text{GeV}^7,\\ |\langle 0|\chi^\dagger\mathcal{K}_{^1D_2}\psi|\eta_{b2}\rangle|^2 &= \frac{5N_c}{8\pi}\overline{\mathcal{R}''_D}(\mu_F)^2\approx\frac{5N_c}{8\pi}\times 0.8394\\ &= 0.5010\ \text{GeV}^7,\end{aligned}\tag{24}$$

where we have approximated the scale-dependent $\overline{\mathcal{R}''_D}(\mu_F)$ with $\mathcal{R}''_D$ from the Cornell potential model [68,69]. The approximation will unavoidably render the decay width to develop a μ_F dependence. Actually, the scale independence can be recovered if we evolute the LDMEs from some scale $m_Q v_Q$ to μ_F by applying the renormalizaiton group, however the manipulation may be questionable due to the evolution in the nonperturbative energy range. Fortunately, as will be found, the decay width is insensitive to the factorization scale, this observation, to some extent, qualifies our approximation in Eq. (24).

With these input parameters, we present our predictions for the decay widths of $\eta_{c2}/\eta_{b2}\to 2\gamma$ at various levels of accuracy in α_s in Table I. The uncertainties affiliated with the decay width are estimated by varying μ_R from m_Q to $2m_Q$ with the central values evaluated at $\sqrt{2}m_Q$.[3] From the table, we have several observations. First, the NNLO decay width is much smaller than the LO one for the channel $\eta_{c2}\to 2\gamma$, which is accounted for by the sizeable and negative $\mathcal{O}(\alpha_s)$ and $\mathcal{O}(\alpha_s^2)$ radiative corrections. Second, the decay width is insensitive to the factorization scale μ_F (we stress that $\mu_F = 1$ GeV may be a little small for perturbative prediction; however, the conclusion will not change by adjusting μ_F). Third, the decay width of $\eta_{b2}\to 2\gamma$ is considerably smaller than the case of η_{c2}, which is mainly caused by the heavier quark mass and smaller electric charge for bottom quark.

We can also predict the branching ratio of $\eta_{Q2}\to 2\gamma$. According to current theoretical computation, η_{c2} decay predominately through the electric $E1$ transition and hadronic decay. If we assume that the η_{Q2} decay is saturated by these two decay patterns, then we can approximate the total decay width through [11]

$$\Gamma_{\text{total}}(\eta_{Q2})\approx\Gamma(\eta_{Q2}\to\text{LH})+\Gamma(\eta_{Q2}\to\gamma h_Q),\tag{25}$$

where LH denotes the abbreviation for light hadrons. The hadronic decay width of η_{Q2} up to NLO has been known for a long time [11], and the prediction for electromagnetic $E1$ transition of $^1D_2\to{}^1P_1$ from Cornell potential model can be found in Refs. [2,8]. Thus, we readily obtain the total decay width $\Gamma_{\text{total}}(\eta_{c2}) = 142.1+303.0 = 445.1$ keV and $\Gamma_{\text{total}}(\eta_{b2}) = 3.8+25.3 = 29.1$ keV, where we have reevaluated the hadronic decay width with the parameters selected in this work. Consequently, the branching ratio of $\eta_{Q2}\to 2\gamma$ is illustrated in Table I. It is significant that $\text{Br}(\eta_{b2}\to 2\gamma)$ is much smaller than $\text{Br}(\eta_c\to 2\gamma)$, which renders the search for η_{b2} through its electromagnetic decay quite challenging.

B. η_{Q2} production at colliders

In the following, we will evaluate the production cross section of η_{Q2} at the B factory and LHC. The η_{c2} associated production with a photon at the B factory has been studied in Ref. [42], and the corresponding cross section at lowest order in α_s expansion is given by

$$\sigma(e^+e^-\to\eta_{c2}+\gamma)=\frac{80\pi\alpha^3e_c^4(1-4m_c^2/s)}{s^2m_c^5}|\mathcal{R}''_D(0)|^2,\tag{26}$$

[3] In this work, we do not consider the uncertainty originating from the heavy quark pole mass, which is expected to be considerably greater than that from varying the renormalization as well as the NRQCD factorization scales. For more discussion about the heavy quark pole mass, we refer the interested readers to Refs. [70–73]

TABLE II. The cross sections of η_{c2} and η_{b2} at the lowest order in α_s expansion at LHCb. By taking the CM colliding energy $\sqrt{s}=7$, 13 TeV, we evaluate the integrated cross sections with η_{Q2} longitudinal rapidity constraint $4.5>y>2$ and transverse momentum P_T cut.

	$\sqrt{s}=7$ TeV			$\sqrt{s}=13$ TeV		
	P_T cut					
σ in unit of nb	$P_T>2m_Q$	$P_T>3m_Q$	$P_T>4m_Q$	$P_T>2m_Q$	$P_T>2m_Q$	$P_T>4m_Q$
$\sigma(pp\to\eta_{c2}+X)$	24.7	5.1	1.4	47.8	10.5	3.0
$\sigma(pp\to\eta_{b2}+X)\times 10^3$	8.7	1.5	0.3	21.5	4.0	1.0

where $\sqrt{s}=10.58$ GeV is the center-of-mass (CM) energy at the B factory. With the aforementioned input parameters, we immediately arrive at $\sigma(e^+e^-\to\eta_{c2}+\gamma)=1.49$ fb. Due to the small cross section and branching ratio, it seems impossible to detect η_{c2} through its electromagnetic decay at the B factory.

Now we turn to the hadron collider LHC, where a greater number of quarkonia can be produced due to the considerable production cross section, e.g., the cross section of η_c can reach around 0.5 μb through single parton scattering [44]. For $pp\to\eta_{Q2}+X$, the differential cross section through single parton scattering can be factorized as

$$\begin{aligned} d\sigma(pp\to\eta_{Q2}+X) &= \sum_{i,j}\int dx_1 dx_2 f_{i/p}(x_1) f_{j/p}(x_2) \\ &\quad\times d\hat{\sigma}(i+j\to c\bar{c}(^1D_2)+X) \\ &\quad\times \frac{|\langle 0|\chi^\dagger \mathcal{K}_{^1D_2}\psi(\mu_F)|\eta_{Q2}\rangle|^2}{m_Q^7}, \end{aligned} \tag{27}$$

where we have neglected the color-octet contribution, $f_{i/p}(x)$ represents the parton distribution function of a proton, and $d\hat{\sigma}$ denotes the partonic cross section. Since the gluon distribution is overwhelming in the proton at small momentum fraction x, we expect that the gluon scattering will denominate the cross section. Thus, it is reasonable for us to consider gluon-gluon partonic scattering to estimate the cross section of η_{Q2}. In addition, we will carry out the partonic cross section $d\hat{\sigma}$ at lowest order in α_s. For concreteness, we consider the production of η_{Q2} at LHCb detector, where a kinematic constraint on the longitudinal rapidity of η_{Q2} $4.5>y>2$ is implemented. We further take a transverse momentum P_T cut for the η_{Q2} to guarantee the validity of the factorization formula (27). In our computation, we employ *CTEQ14* PDF sets [74] for the proton PDF.

In Table II, we present the theoretical predictions for the cross section of η_{Q2} at two benchmark CM energy $\sqrt{s}=7$, 13 TeV with various transverse momentum cutoffs for η_{Q2}. From the table, we find the cross section of η_{b2} is smaller than that of η_{c2} by roughly three order of magnitude. Taking into account the luminosity at LHCb, we can estimate the number of events for η_{Q2} production. With the integrated luminosity $\mathcal{L}=10$ fb^{-1} at each CM energy, there are 10^7–10^8 η_{c2} and 10^4–10^5 η_{b2} event produced at LHCb. Therefore, LHCb will be an ideal platform to probe η_{Q2}. Furthermore, multiplying the branching ratio of $\eta_{Q2}\to 2\gamma$, we predict that there are several hundreds of double-photon events through $pp\to\eta_{c2}\to 2\gamma$, which is a promising channel to probe this undiscovered charmonium. In contrast, the η_{b2} is proved to be hard to detect through its electromagnetic decay at LHCb.

Finally, we must admit that the cross sections for η_{Q2} production at LHCb may be changed by high-order radiative corrections as well as by the contributions from various color-octet components in η_{Q2}, hence the theoretical predictions in Table II are only a rough estimation. In addition, we have set a P_T cut for η_{Q2} to guarantee the validity of Eq. (27); however, a great number of η_{Q2} may be produced in smaller P_T range, therefore the cross sections for η_{Q2} at LHCb may be underestimate.

VI. SUMMARY

Applying the NRQCD factorization formalism, we evaluate the η_{Q2} electromagnetic decay into double photons up to $\mathcal{O}(\alpha_s^2)$ radiative corrections. For the first time, we scrutinize the validity of the NRQCD factorization for D-wave quakonium decay at NNLO. Both the $\mathcal{O}(\alpha_s)$ and $\mathcal{O}(\alpha_s^2)$ corrections to the decay width of $\eta_{Q2}\to 2\gamma$ are negative. Although the radiative corrections to the helicity amplitude are moderate, the corrections change the LO decay width significantly, especially for η_{c2}. By assuming η_{Q2} decay is saturated by the electric $E1$ transition and the hadronic decay, we obtain the branching ratios $\mathrm{Br}(\eta_{c2}\to 2\gamma)\approx 5\times 10^{-6}$ and $\mathrm{Br}(\eta_{b2}\to 2\gamma)\approx 4\times 10^{-7}$. We have also studied the η_{Q2} production at LHCb. By imposing kinematic restriction on the longitudinal rapidity and transverse momentum of η_{Q2}, we predict the cross sections to be 2–50 nb for η_{c2} and 1–22 pb for η_{b2} for various transverse momentum cutoffs. Thus, it is promising to observe η_{c2} through its electromagnetic decay at LHCb, while quite challenging to detect η_{b2} at the current integrated luminosity.

ACKNOWLEDGMENTS

This work is supported by the National Natural Science Foundation of China under Grants No. 11975187 and No. 11965006, and the Natural Science Foundation of ChongQing under Grant No. cstc2019jcyj-msxmX0479.

[1] E. J. Eichten, K. Lane, and C. Quigg, Phys. Rev. D **69**, 094019 (2004).
[2] T. Barnes, S. Godfrey, and E. S. Swanson, Phys. Rev. D **72**, 054026 (2005).
[3] B. Q. Li and K. T. Chao, Phys. Rev. D **79**, 094004 (2009).
[4] S. Godfrey and N. Isgur, Phys. Rev. D **32**, 189 (1985).
[5] L. P. Fulcher, Phys. Rev. D **44**, 2079 (1991).
[6] J. Zeng, J. W. Van Orden, and W. Roberts, Phys. Rev. D **52**, 5229 (1995).
[7] D. Ebert, R. N. Faustov, and V. O. Galkin, Phys. Rev. D **67**, 014027 (2003).
[8] E. J. Eichten, K. Lane, and C. Quigg, Phys. Rev. Lett. **89**, 162002 (2002).
[9] N. Brambilla *et al.* (Quarkonium Working Group), CERN Report No. CERN-2005-005, 2005, https://doi.org/10.5170/CERN-2005-005.
[10] V. A. Novikov, L. B. Okun, M. A. Shifman, A. I. Vainshtein, M. B. Voloshin, and V. I. Zakharov, Phys. Rep. **41**, 1 (1978).
[11] Y. Fan, Z. G. He, Y. Q. Ma, and K. T. Chao, Phys. Rev. D **80**, 014001 (2009).
[12] S. K. Choi *et al.* (Belle Collaboration), Phys. Rev. Lett. **89**, 102001 (2002); **89**, 129901(E) (2002).
[13] K. Chilikin *et al.* (Belle Collaboration), Phys. Rev. D **100**, 012001 (2019).
[14] K. Abe *et al.* (Belle Collaboration), arXiv:hep-ex/0107050.
[15] B. Aubert *et al.* (*BABAR* Collaboration), arXiv:hep-ex/0203040.
[16] B. Aubert *et al.* (*BABAR* Collaboration), Phys. Rev. D **65**, 032001 (2002).
[17] K. W. Edwards *et al.* (CLEO Collaboration), Phys. Rev. Lett. **86**, 30 (2001).
[18] G. T. Bodwin, E. Braaten, and G. P. Lepage, Phys. Rev. D **51**, 1125 (1995); **55**, 5853(E) (1997).
[19] P. w. Ko, J. Lee, and H. S. Song, Phys. Lett. B **395**, 107 (1997).
[20] Y. Fan, J. Z. Li, C. Meng, and K. T. Chao, Phys. Rev. D **85**, 034032 (2012).
[21] H. Xu, X. Liu, and T. Matsuki, Phys. Rev. D **94**, 034005 (2016).
[22] T. Wang, G. L. Wang, W. L. Ju, and Y. Jiang, J. High Energy Phys. 03 (2013) 110.
[23] K. Chilikin *et al.* (Belle Collaboration), J. High Energy Phys. 05 (2020) 034.
[24] M. Tanabashi *et al.* (Particle Data Group), Phys. Rev. D **98**, 030001 (2018).
[25] A. Czarnecki and K. Melnikov, Phys. Rev. Lett. **80**, 2531 (1998).
[26] M. Beneke, A. Signer, and V. A. Smirnov, Phys. Rev. Lett. **80**, 2535 (1998).
[27] A. Czarnecki and K. Melnikov, Phys. Lett. B **519**, 212 (2001).
[28] A. I. Onishchenko and O. L. Veretin, Eur. Phys. J. C **50**, 801 (2007).
[29] P. Marquard, J. H. Piclum, D. Seidel, and M. Steinhauser, Phys. Rev. D **89**, 034027 (2014).
[30] M. Beneke, Y. Kiyo, P. Marquard, A. Penin, J. Piclum, D. Seidel, and M. Steinhauser, Phys. Rev. Lett. **112**, 151801 (2014).
[31] L. B. Chen and C. F. Qiao, Phys. Lett. B **748**, 443 (2015).
[32] W. L. Sang, F. Feng, Y. Jia, and S. R. Liang, Phys. Rev. D **94**, 111501 (2016).
[33] F. Feng, Y. Jia, and W. L. Sang, Phys. Rev. Lett. **115**, 222001 (2015).
[34] L. B. Chen, J. Jiang, and C. F. Qiao, J. High Energy Phys. 04 (2018) 080.
[35] L. B. Chen, Y. Liang, and C. F. Qiao, J. High Energy Phys. 01 (2018) 091.
[36] F. Feng, Y. Jia, and W. L. Sang, Phys. Rev. Lett. **119**, 252001 (2017).
[37] S. Q. Wang, X. G. Wu, W. L. Sang, and S. J. Brodsky, Phys. Rev. D **97**, 094034 (2018).
[38] F. Feng, Y. Jia, and W. L. Sang, arXiv:1901.08447.
[39] B. A. Kniehl, A. V. Kotikov, A. I. Onishchenko, and O. L. Veretin, Nucl. Phys. **B948**, 114780 (2019).
[40] H. M. Yu, W. L. Sang, X. D. Huang, J. Zeng, X. G. Wu, and S. J. Brodsky, J. High Energy Phys. 01 (2021) 131.
[41] W. L. Sang, F. Feng, and Y. Jia, J. High Energy Phys. 10 (2020) 098.
[42] D. Li, Z. G. He, and K. T. Chao, Phys. Rev. D **80**, 114014 (2009).
[43] E. Braaten and J. Lee, Phys. Rev. D **67**, 054007 (2003); **72**, 099901(E) (2005).
[44] H. F. Zhang, Z. Sun, W. L. Sang, and R. Li, Phys. Rev. Lett. **114**, 092006 (2015).
[45] H. E. Haber, arXiv:hep-ph/9405376.
[46] W. L. Sang and Y. Q. Chen, Phys. Rev. D **81**, 034028 (2010).
[47] G. T. Bodwin and A. Petrelli, Phys. Rev. D **66**, 094011 (2002); **87**, 039902(E) (2013).
[48] T. Hahn, Comput. Phys. Commun. **140**, 418 (2001).
[49] R. Mertig, M. Bohm, and A. Denner, Comput. Phys. Commun. **64**, 345 (1991).
[50] V. Shtabovenko, R. Mertig, and F. Orellana, Comput. Phys. Commun. **207**, 432 (2016).
[51] F. Feng and R. Mertig, arXiv:1212.3522.
[52] J. Kuipers, T. Ueda, J. A. M. Vermaseren, and J. Vollinga, Comput. Phys. Commun. **184**, 1453 (2013).

[53] F. Feng, Comput. Phys. Commun. **183**, 2158 (2012).
[54] A. V. Smirnov, Comput. Phys. Commun. **189**, 182 (2015).
[55] R. Cools and A. Haegemans, ACM Trans. Math. Softw. **29**, 287 (2003).
[56] https://github.com/stevengj/cubature, HCubature web site.
[57] S. Borowka and G. Heinrich, *Proc. Sci.*, LL2012 (2012) 037 [arXiv:1209.6345].
[58] D. J. Broadhurst, N. Gray, and K. Schilcher, Z. Phys. C **52**, 111 (1991).
[59] K. Melnikov and T. van Ritbergen, Nucl. Phys. **B591**, 515 (2000).
[60] P. Bärnreuther, M. Czakon, and P. Fiedler, J. High Energy Phys. 02 (2014) 078.
[61] A. H. Hoang and P. Ruiz-Femenia, Phys. Rev. D **74**, 114016 (2006).
[62] A. V. Manohar and I. W. Stewart, Phys. Rev. D **62**, 014033 (2000).
[63] A. H. Hoang, Phys. Rev. D **69**, 034009 (2004).
[64] A. H. Hoang and P. Ruiz-Femenia, Phys. Rev. D **73**, 014015 (2006).
[65] A. Pineda, Phys. Rev. D **65**, 074007 (2002).
[66] K. G. Chetyrkin, J. H. Kuhn, and M. Steinhauser, Comput. Phys. Commun. **133**, 43 (2000).
[67] J. Erler, Phys. Rev. D **59**, 054008 (1999).
[68] E. J. Eichten and C. Quigg, Phys. Rev. D **52**, 1726 (1995).
[69] E. J. Eichten and C. Quigg, arXiv:1904.11542.
[70] P. Marquard, A. V. Smirnov, V. A. Smirnov, and M. Steinhauser, Phys. Rev. Lett. **114**, 142002 (2015).
[71] A. L. Kataev and V. S. Molokoedov, Eur. Phys. J. Plus **131**, 271 (2016).
[72] C. Ayala, X. Lobregat, and A. Pineda, Phys. Rev. D **101**, 034002 (2020).
[73] V. Mateu and P. G. Ortega, J. High Energy Phys. 01 (2018) 122.
[74] S. Dulat, T. J. Hou, J. Gao, M. Guzzi, J. Huston, P. Nadolsky, J. Pumplin, C. Schmidt, D. Stump, and C. P. Yuan, Phys. Rev. D **93**, 033006 (2016).